

Real-Time Imaging of Crystallization in Polylactide Enantiomeric Monolayers at the Air–Water Interface

Young Shin Kim,[†] Christopher M. Snively,^{†,‡} Yujuan Liu,^{†,||} John F. Rabolt,^{*,†} and D. Bruce Chase[§]

Department of Materials Science and Engineering, Department of Chemical Engineering, University of Delaware, Newark, Delaware 19716, and Central Research and Development, DuPont Experimental Station, Wilmington, Delaware 19880-0328

Received November 22, 2007. Revised Manuscript Received July 14, 2008

A newly developed planar array infrared reflection–absorption spectrograph (PA-IRRAS) offers significant advantages over conventional approaches including fast acquisition speed, excellent compensation for water vapor, and an excellent capacity for large infrared accessories, e.g., a water trough. In this study, the origin of stereocomplexation in a polylactide enantiomeric monolayer at the air–water interface was investigated using PA-IRRAS. PA-IRRAS was used as a probe to follow the real-time conformational changes associated with intermolecular interactions of polymer chains during the compression of the monolayers. It was found that a mixture of poly(D-lactic acid) (PDLA) and poly(L-lactic acid) (PLLA) (D/L) formed a stereocomplex when the two-dimensional monolayer developed at the air–water interface before film compression, indicating that there is no direct correlation between film compression and stereocomplexation. PA-IRRAS spectra of the stereocomplex exhibited distinct band shifts in crystalline sensitive components, e.g., the $\nu_{as}(\text{C}-\text{O}-\text{C}, \text{h})$ mode, as well as amorphous-dependent components, e.g., the $\nu_s(\text{C}-\text{O}-\text{C})$ mode, when compared with the spectra of PLLA alone. On the other hand, time-resolved PA-IRRAS spectra, which were obtained as the films were being compressed, revealed that both monolayers of PLLA and mixed PLLA/PDLA stereocomplex were crystallized into a 10_3 -helix and a 3_1 -helix, respectively, with a distinct band shift in crystalline sensitive components only. Fourier self-deconvolution of the spectra demonstrated that the band shift in crystalline sensitive components is correlated with the intermolecular interaction of polymer chains.

Introduction

Poly(lactic acid) (PLA) is of great interest in a variety of research applications including use as a drug carrier¹ and in the form of electrospun nanofibers² as a scaffold for tissue regeneration.³ PLA, which is biodegradable, biocompatible, easily processable and exhibits excellent mechanical properties, can be synthesized via ring opening or condensation polymerization and forms either optically active homopolymers with a D or L chiral unit, or as copolymers with both D and L chiral units.⁴ Physical properties of PLA vary with the chiral unit distribution, crystallinity, and tacticity, which also affect the biological properties and the kinetics of the degradation of the polymers.^{5–8} In addition, a mixture of optically active homopolymers, poly(D-lactic acid) (PDLA) and poly(L-lactic acid) (PLLA), exhibits unique physical properties when compared with those of the

pure polymers. In 1986, Ikada et al.⁹ first reported stereocomplexation of this mixed polymer system, which exhibits a higher melting point and change of crystal structure compared to the pure polymeric enantiomers due to additional intermolecular interactions.

Stereocomplexation of a mixed PDLA/PLLA system occurs when it is crystallized from the melt or solution and this leads to a less dense unit cell ($1.24 \text{ g} \cdot \text{mL}^{-1}$) than for the pure polymer ($1.29 \text{ g} \cdot \text{mL}^{-1}$).^{10–12} Generally, PDLA and PLLA adopt a right-handed and a left-handed helix, respectively, both adopting a 10_3 -helical structure.^{9,13} In the stereocomplex, the two types of helical structures facilitate the interaction between opposing oxygen atoms and hydrogen atoms via the stereoselective van der Waals force, which leads to close packing and the formation of a 3_1 -helical structure.¹³ In addition, since the formation of the stereocomplex is related to the competition between favorable van der Waals force and unfavorable entropy in polymer chains, the complexation can be affected by several factors, e.g., higher molar mass and molar mass distribution, and imperfect mixing.¹³ Besides the PLA system, other polymer systems can undergo stereocomplexation, including poly(methyl methacrylate) (PMMA),¹⁴ α -methylbenzyl methacrylate,¹⁵ poly(*t*-butyl thiirane),¹⁵ poly(benzyl glutamate),¹⁶ and poly(α -methyl α -ethyl β -propiolactone).¹⁷

* To whom correspondence should be addressed. Tel: (302) 831-4476. Fax: (302) 831-4545. E-mail: rabolt@udel.edu.

[†] Department of Materials Science and Engineering, University of Delaware.

[‡] Department of Chemical Engineering, University of Delaware.

[§] DuPont Experimental Station.

^{||} Current address: Research and Development Center, Grace Construction Products, Grace China, Beijing, China, 100176.

(1) Saito, N.; Okada, T.; Horiuchi, H.; Murakami, N.; Takahashi, J.; Nawata, M.; Ota, H.; Nozaki, K.; Takaoka, K. *Nat. Biotechnol.* **2001**, *19*, 332.

(2) Sun, Z. C.; Zussman, E.; Yarin, A. L.; Wendorff, J. H.; Greiner, A. *Adv. Mater.* **2003**, *15*, 1929.

(3) Huang, C. K.; Huang, W.; Heiden, K.; Jarrahy, R.; Zuk, P.; Rudkin, G.; Ishida, K.; Yamaguchi, D.; Miller, T. A. *J. Bone Miner. Res.* **2006**, *21*, S343.

(4) Braun, B.; Dorgan, J. R.; Dec, S. F. *Macromolecules* **2006**, *39*, 9302.

(5) Chabot, F.; Vert, M.; Chapelle, S.; Granger, P. *Polymer* **1983**, *24*, 53.

(6) Schindler, A.; Harper, D. *J. Polym. Sci. Pol. Lett.* **1976**, *14*, 729.

(7) Thakur, K. A. M.; Kean, R. T.; Zupfer, J. M.; Buehler, N. U.; Doscotch, M. A.; Munson, E. *J. Macromolecules* **1996**, *29*, 8844.

(8) Cassanas, G.; Kister, G.; Fabrègue, E.; Morssli, M.; Bardet, L. *Spectrochim. Acta A* **1993**, *49*, 271.

(9) Ikada, Y.; Jamshidi, K.; Tsuji, H.; Hyon, S. H. *Macromolecules* **1987**, *20*, 904.

(10) Tsuji, H.; Hyon, S. H.; Ikada, Y. *Macromolecules* **1991**, *24*, 5657.

(11) Tsuji, H.; Hyon, S. H.; Ikada, Y. *Macromolecules* **1991**, *24*, 5651.

(12) Eling, B.; Gogolewski, S.; Pennings, A. *J. Polymer* **1982**, *23*, 1587.

(13) Slager, J.; Domb, A. *J. Adv. Drug Delivery Rev.* **2003**, *55*, 549.

(14) Liquori, A. M.; Anzuino, G.; Coiro, V. M.; Dalagni, M.; Desantis, P.; Savino, M. *Nature (London)* **1965**, *206*, 358.

(15) Dumas, P.; Spassky, N.; Sigwalt, P. *Makromol. Chem.* **1972**, *156*, 65.

(16) Fukuzawa, T.; Uematsu, I. *Polym. J. (Tokyo)* **1974**, *6*, 537.

(17) Lavalée, C.; Prudhomme, R. E. *Macromolecules* **1989**, *22*, 2438.

The PDLA/PLLA system has been actively studied in a two-dimensional (2-D) format such as a monolayer. It was found that a monolayer of mixed PDLA/PLLA also forms a stereocomplex at the air–water interface as reported by Klass et al.¹⁸ This was demonstrated by the appearance of a specific feature in the surface pressure–area isotherm when compared with that of the pure polymer, obtained via a Wilhelmy balance. Polarization modulation infrared reflection–absorption spectroscopy (PM-IRRAS) was also used to investigate the conformational structure of the stereocomplex formed in a PDLA/PLLA monolayer at the air–water interface. Although Pelletier et al.¹⁹ demonstrated that stereocomplexation could be induced by the compression of the PLA enantiomeric monolayer at the air–water interface, the precise mechanism of stereocomplexation in a 2-D monolayer system remains a topic of active investigation.

Monolayers on the water subphase, including Langmuir–Blodgett (LB) films, have been widely characterized via external infrared reflection–absorption spectroscopy (IRRAS).²⁰ The major problems encountered when acquiring structural information from a monolayer at the air–water interface via IRRAS are the poor infrared reflectivity of water and the spectral interference by the infrared absorption of water. Since Dluhy and co-workers reported the feasibility of obtaining spectra from various types of phospholipids at the air–water interface, notable improvements in IRRAS have been made.^{21,22} Gericke et al.²³ reported that the IR absorption of water vapor can be minimized by using dry nitrogen gas at a low flow rate in the sampling chamber. Flach et al.^{24,25} demonstrated that the IR absorption of water vapor can be effectively subtracted by the use of an IRRAS sampling accessory, in which a miniaturized water trough, divided into two wells for sample and reference, was moved back and forth repeatedly after a preset number of scans. Additionally, with a PM-IRRAS instrument, these problems are minimized because the instrument employs a modulated polarized IR signal and consequently the resulting polarization modulated reflectivity is independent of isotropic absorbance, thus allowing suppression of water vapor signals.^{26–28} However, this could be a disadvantage in that the isotropic absorption bands of interest are also not observed.²⁹ Another important issue for these FTIR-based techniques is the relatively long data acquisition time, which is required. For instance, when spectra from a monolayer during compression are acquired using these instruments, the barrier of the trough, which compresses the film, must be stopped for a considerable time period during the collection of each data point. During this time period, structural rearrangement of the monolayer is possible. Therefore, using results from such an FTIR based experiment, it would be difficult to fully discuss the dynamics of the film formation mechanism.

Planar array infrared (PA-IR) spectroscopy has significant advantages over conventional FTIR instruments including a rapid data acquisition (maximum temporal resolution of $<100\ \mu\text{s}$) and excellent sensitivity.^{30–32} In addition, a newly developed accessory for planar array infrared reflection–absorption spectroscopy (PA-IRRAS) can record the sample and reference spectra simultaneously, allowing the real-time background correction and compensation for the IR absorption of water.³³ In this study, real-time spectra of PLA enantiomeric monolayers and PLLA/PDLA mixtures at the air–water interface ($1800\text{--}1000\ \text{cm}^{-1}$) were obtained via PA-IRRAS as the films were being compressed. With this result, the origin of PLA stereocomplexation and the kinetics of PLA crystallization induced by the compression process are discussed.

Experimental Section

Langmuir Film Measurement. Surface pressure–area ($\pi\text{--}A$) isotherms of PLA monolayers were obtained via a Wilhelmy balance, which is equipped with a water trough, a single barrier, and a filter paper Wilhelmy plate (Mini trough system 2, KSV Instruments Ltd., Helsinki, Finland). The water trough was filled with deionized (DI) water ($18.2\ \text{M}\Omega\text{-cm}$, Nanopure Diamond, Barnstead) as a subphase. The temperature of the water trough was maintained at $20\ ^\circ\text{C}$ using a water circulator (Isotemp 3016, Fisher Scientific). For the sample preparation, PDLA ($M_n = 13\ 800\ \text{g}\cdot\text{mol}^{-1}$, PDI = 1.19) and PLLA ($M_n = 14\ 000\ \text{g}\cdot\text{mol}^{-1}$, PDI = 1.12) were purchased from Polymer Source (Dorval, Canada) and used without further purification. The polymer was dissolved into chloroform (Sigma) at a concentration of $0.2\ \text{mg}\cdot\text{mL}^{-1}$. The polymer solution ($25\text{--}50\ \mu\text{L}$) was spread over the water surface and compressed at a compression rate of $5\ \text{mm}\cdot\text{min}^{-1}$ after a delay of 15 min to allow the evaporation of the solvent.

Planar Array Infrared Reflection–Absorption Spectra. The PA-IRRAS experimental setup has been described in detail elsewhere.³³ Briefly, the water trough, which was divided into two wells for sample and reference, was filled with DI water (approximately 70 mL for each well).³³ To obtain PA-IRRAS absorbance spectra, a dark background was acquired first by blocking the optical path at the sample holder. A background scan for sample and reference channels was acquired from both wells of the water trough. Then, the solution of PLLA or D/L mixture (50/50, v/v) at $0.2\ \text{mg}\cdot\text{mL}^{-1}$ ($40\text{--}60\ \mu\text{L}$) was spread over the sample well only. After a delay of 15 min to allow solvent evaporation, sample spectra for sample and reference channels were continuously acquired from both wells simultaneously during the compression of the films using a compression rate of $5\ \text{mm}\cdot\text{min}^{-1}$. Absorbance spectra for sample and reference were calculated using Matlab software (Matlab 7.0, The MathWorks, Inc.). The water bands were compensated for by ratioing sample spectra to reference spectra as described previously.³³ The frame rate and integration time of the FPA were 115 Hz and $113\ \mu\text{s}$, respectively. Each spectrum is the result of averaging 10 sets of 100 frames, and required a total acquisition time of 10.8 s (total integration time: 1.5 s). A plane ruled diffraction grating ($50\ \text{groove}\cdot\text{mm}^{-1}$, SPEX, Edison, NJ) and a mercury cadmium telluride focal plane array (MCT FPA, 256×256 pixels, Santa Barbara Focal plane, CA) detector were used to obtain PA-IRRAS spectra in the spectral range of $1800\text{--}1000\ \text{cm}^{-1}$. The temperature of the water trough was maintained at $20\ ^\circ\text{C}$ for all experiments. The enclosure housing for the PA-IRRAS instrument was purged with dry nitrogen gas from a purge gas generator (Parker filtration, MA) to maintain relative humidity at 14–16%. All spectra were obtained at an incident

(18) Klass, J. M.; Lennox, R. B.; Brown, G. R.; Bourque, H.; P  zolet, M. *Langmuir* **2003**, *19*, 333.

(19) Pelletier, I.; P  zolet, M. *Macromolecules* **2004**, *37*, 4967.

(20) Ulman, A. *Ultrathin Organic Films*; Academic press: San Diego, 1991.

(21) Dluhy, R. A.; Cornell, D. G. *J. Phys. Chem.* **1985**, *89*, 3195.

(22) Hunt, R. D.; Mitchell, M. L.; Dluhy, R. A. *J. Mol. Struct.* **1989**, *214*, 93.

(23) Gericke, A.; Michailov, A. V.; Huhnerfuss, H. *Vib. Spectrosc.* **1993**, *4*, 335.

(24) Flach, C. R.; Brauner, J. W.; Mendelsohn, R. *Appl. Spectrosc.* **1993**, *47*, 982.

(25) Flach, C. R.; Brauner, J. W.; Taylor, J. W.; Baldwin, R. C.; Mendelsohn, R. *Biophys. J.* **1994**, *67*, 402.

(26) Blaudez, D.; Buffeteau, T.; Cornut, J. C.; Desbat, B.; Escafre, N.; P  zolet, M.; Turlet, J. M. *Appl. Spectrosc.* **1993**, *47*, 869.

(27) Blaudez, D.; Buffeteau, T.; Cornut, J. C.; Desbat, B.; Escafre, N.; P  zolet, M.; Turlet, J. M. *Thin Solid Films* **1994**, *242*, 146.

(28) Blaudez, D.; Turlet, J. M.; Dufourcq, J.; Bard, D.; Buffeteau, T.; Desbat, B. *J. Chem. Soc., Faraday Trans.* **1996**, *92*, 525.

(29) Mendelsohn, R.; Brauner, J. W.; Gericke, A. *Annu. Rev. Phys. Chem.* **1995**, *46*, 305.

(30) Elmore, D. L.; Tsao, M. W.; Frisk, S.; Chase, D. B.; Rabolt, J. F. *Appl. Spectrosc.* **2002**, *56*, 145.

(31) Pellerin, C.; Snively, C. M.; Chase, D. B.; Rabolt, J. F. *Appl. Spectrosc.* **2004**, *58*, 639.

(32) Pelletier, I.; Pellerin, C.; Chase, D. B.; Rabolt, J. F. *Appl. Spectrosc.* **2005**, *59*, 156.

(33) Kim, Y. S.; Snively, C. M.; Chase, D. B.; Rabolt, J. F. *Appl. Spectrosc.* **2007**, *61*, 916.

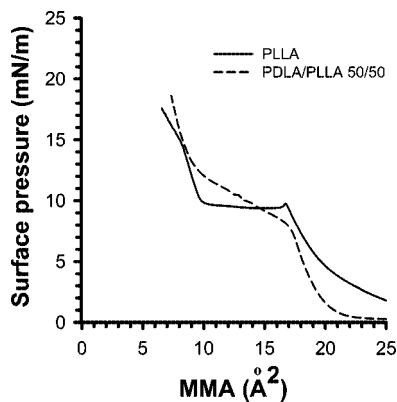


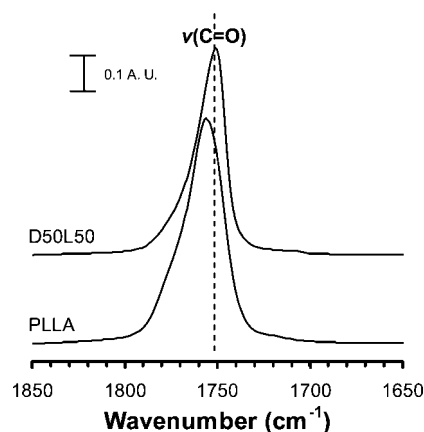
Figure 1. Surface pressure–area isotherms of the pure polymer (PLLA) and the mixed PDLA/PLLA (50/50) at the air–water interface at 20 °C. MMA: mean molecular area ($\text{\AA}^2/\text{repeat unit}$).

angle of 45–50°. Fourier self-deconvolution for the $\nu_{as}(\text{C–O–C})$ mode of the ester group was carried out using OMNIC software (Thermo Nicolet Co.) to determine the band shift during the compression process.

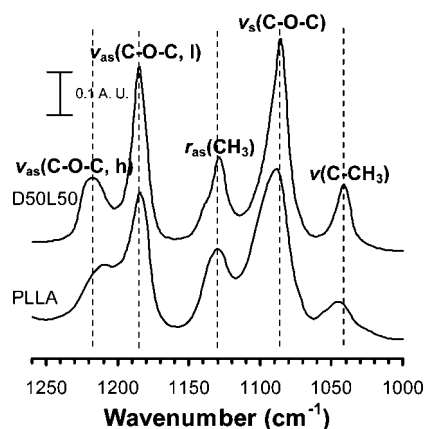
Attenuated Total Reflection Spectra. Twenty microliters of PLLA or D/L mixture solutions at $0.2 \text{ mg}\cdot\text{mL}^{-1}$ were placed onto a diamond window of an ATR accessory (DurasamplIR II, SENSIR, CT) and allowed to dry. ATR spectra were obtained at 4 cm^{-1} resolution using a Nexus 670 FTIR (Thermo Nicolet, WI) equipped with an MCT detector.

Results and Discussion

Intermolecular Interaction of PLA Monolayers at the Air–Water Interface. Figure 1 shows surface pressure–area (π – A) isotherms of PLLA and mixed D/L films on a water subphase at 20 °C. The important features of the π – A isotherms can be related to the intermolecular interaction between the molecules, the phase of the PLA film, and the rate of nucleation and crystallization. In the preplateau region, compression of the PLLA film leads to an increase in the surface pressure. However, the surface pressure for the mixed polymer film did not increase until an area of $23 \text{ \AA}^2/\text{repeat unit}$ was reached and then it displayed a rapid rise. One possible reason for this is the incompressibility of the mixed polymer film. The features in the preplateau region suggest that the PLLA film is compressible, while the mixed polymer film is stiffer presumably as a result of the stereocomplexation. A plateau in the isotherm for PLLA, which is characteristic of a first-order thermodynamic transition, is related to the equilibrium of solid and liquid phases. In this region, compression does not contribute to the surface pressure, indicating that a low level of van der Waals interaction between the molecules in the film exists.³⁴ This feature can also be observed in short-chain fatty acids,³⁵ where the plateau region is sensitive to the length of the hydrocarbon chain of the fatty acid molecules. Longer hydrocarbon chains, which form higher ordered structures than shorter chains, exhibit an obscured plateau region while fatty acids with shorter chains clearly display a plateau in their π – A isotherm. After this transition, the surface pressure rapidly increases due to the formation of a solid-like film.¹⁹ For the mixed polymer film, the knee in the π – A isotherm was less well defined and the plateau was not observed, indicative of a stronger van der Waals interaction between the molecules, resulting in the formation of a stereocomplex. This interaction made the film



(a)



(b)

Figure 2. ATR-FTIR spectra obtained from solvent cast films of the pure polymer (PLLA) and the D/L mixed polymer in the spectral range of (a) 1850–1650 and (b) 1270–1000 cm^{-1} .

stiffer, giving rise to an increase in surface pressure, and explains why π kept increasing in the region of $9\text{--}17 \text{ \AA}^2/\text{repeat unit}$.

Spectral Characterization of Stereocomplexation in PLA Solvent Cast Films. In order to determine the spectral characteristics of the crystal structure of PLLA and the D/L mixture, IR spectra were obtained from solvent cast films using ATR-FTIR (Figure 2). The observed frequencies and their assignments are listed in Table 1.³⁶ ATR spectra of PDLA and PLLA were similar due to their identical chemical compositions (data not shown). The spectrum of the D/L film, however, revealed considerable band shifts when compared to those of the pure polymers. The bands at 1757 ($\nu(\text{C=O})$), 1208 ($\nu_{as}(\text{C–O–C}, \text{h}, \text{higher frequency})$), 1089 ($\nu_s(\text{C–O–C})$), and 1046 ($\nu(\text{C–CH}_3)$) cm^{-1} in the homopolymer films shift to 1750, 1214, 1085, and 1040 cm^{-1} , respectively, in the mixed polymer. The asymmetric C–O–C mode in PLLA has two components: the $\nu_{as}(\text{C–O–C}, \text{h}, \text{higher frequency})$ and the $\nu_{as}(\text{C–O–C}, \text{l}, \text{lower frequency})$ at c.a. 1208 and 1183 cm^{-1} , respectively, due to significant intermolecular interaction between polymer chains.³⁷ The band split was more clearly seen in the D/L mixture film due to the stronger intermolecular interaction present in the stereocomplex. In this study, we mainly focused on the $\nu_{as}(\text{C–O–C}, \text{h})$ and the

(34) Petty, M. C. *Langmuir–Blodgett films*; Cambridge University Press: New York, 1996.

(35) Pallas, N. R.; Pethica, B. A. *Langmuir* **1985**, *1*, 509.

(36) Bourque, H.; Laurin, I.; P  zolet, M.; Klass, J. M.; Lennox, R. B.; Brown, G. R. *Langmuir* **2001**, *17*, 5842.

(37) Krikorian, V.; Pochan, D. J. *Macromolecules* **2005**, *38*, 6520.

Table 1. Measured IR Frequencies and Assignments for Solvent Cast Films and Langmuir Films of the PLA Pure Polymer and the Mixed PDLA/PLLA

ATR-FTIR (solvent cast film) ³⁶		PA-IRRAS (Langmuir film) ^d		assignment
pure polymer/cm ⁻¹	mixture/cm ⁻¹	pure polymer/cm ⁻¹	mixture/cm ⁻¹	
1046	1040	1045	1038	$\nu(\text{C}-\text{CH}_3)$
1089	1085	1089	1084	$\nu_s(\text{C}-\text{O}-\text{C})$
1129	1128	1132	1130	$r_{\text{as}}(\text{CH}_3)$
1183	1184	1185	1185	$\nu_{\text{as}}(\text{C}-\text{O}-\text{C}, \text{l})$
1208	1214	1209	1216	$\nu_{\text{as}}(\text{C}-\text{O}-\text{C}, \text{h})$
1267	1266	1269	—	$\delta(\text{CH}) + \nu(\text{C}-\text{O}-\text{C})$
1303	1305	—	—	$\delta(\text{CH})$
1366	1367	1368	1368	$\delta(\text{CH}) + \delta_s(\text{CH}_3)$
1383	1383	1383	1384	$\delta_s(\text{CH}_3)$
1455	1456	1454	1456	$\delta_{\text{as}}(\text{CH}_3)$
1757	1750	1756	1751	$\nu(\text{C}=\text{O})$

^a Band positions of the PLA films at the air–water interface at an MMA of about 7 Å²/repeat unit. s = symmetric; as = asymmetric.

$\nu_s(\text{C}-\text{O}-\text{C})$ modes because these components displayed a distinct blue and red shift, respectively, when PDLA was mixed with PLLA. Thus, the observed shift of these two components is considered characteristic of the formation of a stereocomplex. The difference between the $\nu_{\text{as}}(\text{C}-\text{O}-\text{C}, \text{h})$ and the $\nu_s(\text{C}-\text{O}-\text{C})$ modes was 119 and 129 cm⁻¹ for the PLLA and D/L films, respectively. One of the reasons for this spectral difference is the conformational and crystal structure in the mixed polymer film relative to the pure components. It is widely known that PLLA (or PDLA) crystallizes into a 10₃-helix^{38,39} while the D/L mixture adopts a 3₁-helix in either a parallel or antiparallel orientation.⁴⁰ However, in chloroform solution, the band shifts were not observed (data not shown), indicating that the stereocomplexation between PDLA and PLLA is mainly due to contributions from intermolecular interactions rather than intramolecular interactions.

Spectral Characterization of Stereocomplexation in PLA Monolayers at the Air–Water Interface. Although PA-IRRAS has significant advantages over conventional FTIR approaches when spectra are acquired from PLA thin films at the air–water interface during compression of the film, the signal-to-noise ratio (SNR) can be considerably lower than that seen for static films due to sample changes during the collection time, fluctuations of the water surface, and the low level of reflected IR intensity. To improve SNR, multiple-row binning, the process of averaging data from multiple rows of the FPA, was utilized in this study. The PA-IRRAS spectra shown in Figure 3 were acquired from PLLA films at the air–water interface at a maximum mean molecular area (MMA) of ca. 7 Å²/repeat unit during compression of the film. When spectra were acquired with 4000 frames (4 rows upper trace), it was difficult to accurately determine the band position and band shape characteristic of the polymer. These features were more clearly seen in spectra acquired with 20 000 frames (20 rows middle trace). The peak-to-peak noise of spectra acquired with pixel binning of 4 rows and 20 rows was approximately 6×10^{-3} absorbance units (A.U.) and 1.5×10^{-3} A.U., respectively. This means that the pixel binning process effectively reduced the noise level. Therefore, in the experiments involving film compression, all spectra were acquired with 20 000 frames. When this level of signal averaging was employed, the band shifts due to stereocomplexation are clearly visible for the PLLA/PDLA mixture (Figure 3, lower trace).

Figure 4 shows time-resolved PA-IRRAS spectra of a PLLA Langmuir film on the water surface during film compression. The total measurement time for this experiment was ap-

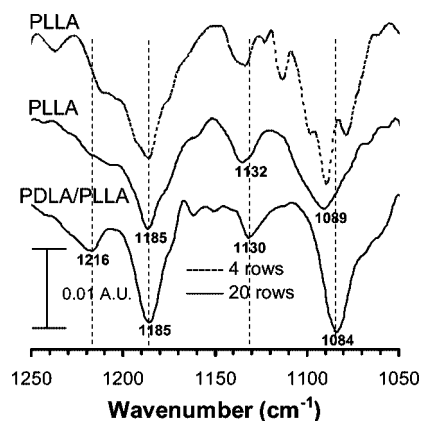


Figure 3. PA-IRRAS spectra of PLLA and D/L mixture thin films at the air–water interface at an MMA of ca. 7 Å²/repeat unit during compression of the films. Spectra were the result of 4 (—) and 20 (—) rows of coadded spectra; upper trace: PLLA (4 rows); middle trace: PLLA (20 rows); and lower trace: PDLA/PLLA (20 rows).

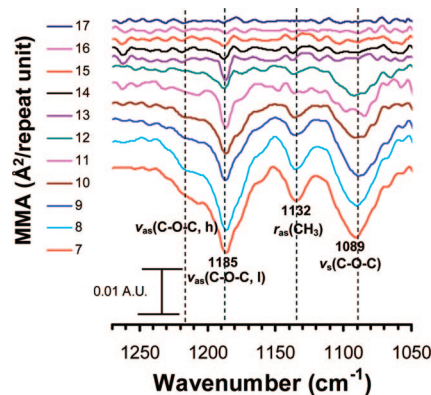


Figure 4. PA-IRRAS spectra of the PLLA Langmuir film at the air–water interface as a function of MMA during the compression process.

proximately 16 min, with each spectrum being acquired at a different MMA in the 10 s measurement time during continuous compression of the films. At an MMA higher than 17 Å², no important spectral features were observed in the PA-IRRAS spectra (data not shown). At an MMA of 9–17 Å², only the weak $\nu_{\text{as}}(\text{C}-\text{O}-\text{C}, \text{l})$ and $\nu_s(\text{C}-\text{O}-\text{C})$ bands were observed due to the low surface density of the film. As the film was further compressed, the absorbance of all IR bands became stronger due to crystallization as well as an increase in surface density of the film. The PA-IRRAS spectra of the PLLA Langmuir film became identical to that of the solvent cast film of PLLA, measured via

(38) Desantis, P.; Kovacs, A. J. *Biopolymers* **1968**, *6*, 299.

(39) Hoogsteen, W.; Postema, A. R.; Pennings, A. J.; Tenbrinke, G.; Zugenmaier, P. *Macromolecules* **1990**, *23*, 634.

(40) Okihara, T.; Tsuji, M.; Kawaguchi, A.; Katayama, K.; Tsuji, H.; Hyon, S. H.; Ikada, Y. *J. Macromol. Sci. Phys.* **1991**, *B30*, 119.

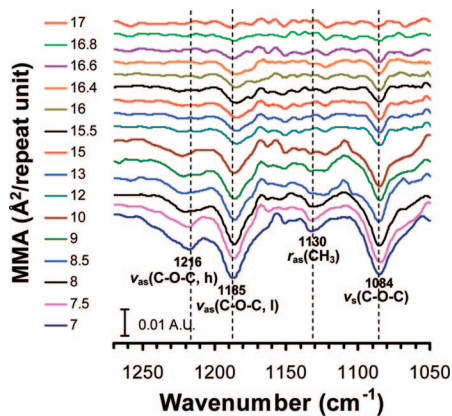


Figure 5. PA-IRRAS spectra of the D/L mixture Langmuir film at the air-water interface as a function of MMA during the compression process.

ATR-FTIR (Figure 2b). This result suggests that the PLLA Langmuir film adopts a 10_3 -helical structure.

Time-resolved spectra of the mixed D/L Langmuir film were also acquired via PA-IRRAS (Figure 5). Unlike PLLA spectra, significant band shifts were observed during compression of the mixed D/L film. At MMA values greater than 17 \AA^2 , no spectral features were observed (data not shown). At an MMA of $9\text{--}17 \text{ \AA}^2$, important changes in the $r_{as}(\text{CH}_3)$, the $\nu_s(\text{C-O-C})$, and the $\nu_{as}(\text{C-O-C, h and l})$ modes were observed, indicating an increase in the surface density of the film. As the film was further compressed, a distinct red shift in the $\nu_{as}(\text{C-O-C, h})$ mode of about 7 cm^{-1} was observed (from 1223 to 1216 cm^{-1}), and the spectra became identical to those of a solvent cast film of the mixed D/L, measured via ATR-FTIR (Figure 2b), indicating the formation of a 3_1 -helical structure.

A comparison of the PA-IRRAS spectra of PLLA and mixed D/L Langmuir films is shown in Figure 3. Both spectra were acquired at an MMA of approximately 7 \AA^2 during compression of the film. As observed in the ATR-FTIR result, the PA-IRRAS spectrum of the mixed polymer film revealed distinct blue and red shifts in the $\nu_{as}(\text{C-O-C, h})$ and the $\nu_s(\text{C-O-C})$ modes, respectively, when compared to the pure polymer spectrum. In addition, the shift in the $\nu_{as}(\text{C-O-C, h})$ mode was pronounced. These results clearly indicate that the mixed D/L film adopted the 3_1 -helical structure and formed a stereocomplex at the air-water interface.⁹⁻¹³

Crystallization of PLA Enantiomeric Monolayers during Film Compression. As mentioned above, during the compression process, the mixed D/L Langmuir film displayed a distinct red shift in the $\nu_{as}(\text{C-O-C, h})$ mode while this was not clearly observed for the pure polymer (Figure 4 and 5). This result leads us to an interesting question: what is the origin of the band shift during film compression? For this question, the C-O-C vibrational modes were analyzed in detail. As shown in Figure 2 and 3, the mixing process of PDLA and PLLA leads to significant band shifts in the $\nu_{as}(\text{C-O-C, h})$ and $\nu_s(\text{C-O-C})$ modes compared to that of the PLLA film. However, during the compression of the mixed D/L Langmuir film (Figure 5), only a red shift in the $\nu_{as}(\text{C-O-C, h})$ mode was observed without a significant band shift in the $\nu_s(\text{C-O-C})$ mode. This observation is not consistent with the band shift occurring in the formation of a stereocomplex. Therefore, it is hypothesized that the origin of the band shift during the compression process is film crystallization rather than stereocomplexation. Previous work by Krikorian et al. demonstrated that in the study of crystallization kinetics of PLLA, the $\nu_{as}(\text{C-O-C, h})$ mode is crystalline sensitive

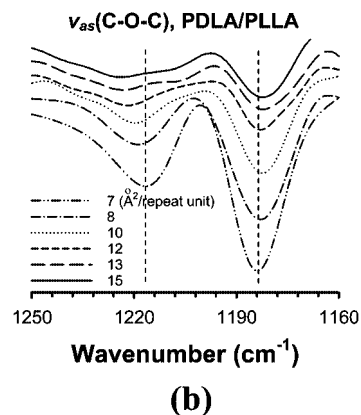
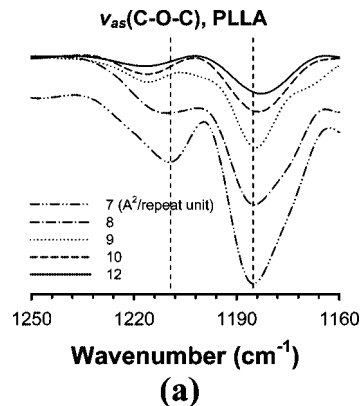


Figure 6. Fourier self-deconvolution of the $\nu_{as}(\text{C-O-C, h and l})$ mode of (a) the PLLA Langmuir film and (b) the D/L mixture Langmuir film during the compression process.

and the $\nu_{as}(\text{C-O-C, l})$ and the $\nu_s(\text{C-O-C})$ modes are amorphous-dependent.³⁷ Since, the $\nu_{as}(\text{C-O-C, h})$ mode in the D/L mixed monolayer displayed a distinct red shift while the $\nu_{as}(\text{C-O-C, l})$ and the $\nu_s(\text{C-O-C})$ modes did not shift during the compression process this observation supports the hypothesis of crystallization during film compression. In addition, further spectral analysis was carried out using Fourier self-deconvolution to see if there are red shifts in the $\nu_{as}(\text{C-O-C, h})$ mode of both PLLA and D/L Langmuir films during the film compression, which is indicative of the crystallization of PLA. As a result of the deconvolution, the red shift of the $\nu_{as}(\text{C-O-C, h})$ mode was observed in both Langmuir films (Figure 6). Therefore, it is concluded that the band shift during the compression process is related to crystallization of the films rather than stereocomplexation.

The band positions of the $\nu_{as}(\text{C-O-C, h})$ mode for PLLA and the D/L mixture Langmuir films were plotted as a function of MMA to follow conformational changes in the polymer backbone during the compression process (Figure 7). Similar approaches have been used in other studies which describe the kinetics of conformational changes during the crystallization of PLLA.^{37,41,42} In these studies, it was found that changes in the $\nu_{as}(\text{C-O-C, h})$ mode could be ascribed to the intermolecular interaction of polymer chains during the formation of the 10_3 -helical structure. Due to this reason, the conformational changes in the D/L Langmuir film displayed a different behavior than that observed for a PLLA film. For instance, for PLLA, the

(41) Zhang, J. M.; Tsuji, H.; Noda, I.; Ozaki, Y. *Macromolecules* **2004**, *37*, 6433.

(42) Zhang, J. M.; Tsuji, H.; Noda, I.; Ozaki, Y. *J. Phys. Chem. B* **2004**, *108*, 11514.

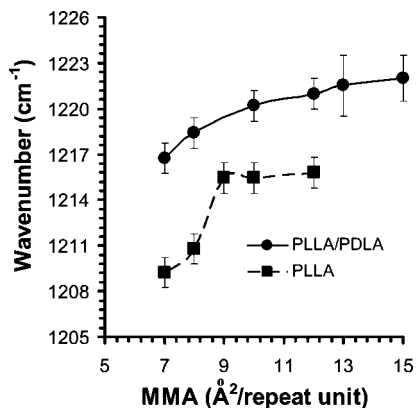


Figure 7. Band position of the $\nu_{as}(\text{C-O-C, h})$ mode of the PLLA and the D/L mixture Langmuir films as a function of MMA during the compression process.

conformational changes occurred rapidly at $<9 \text{ \AA}^2$ MMA, where the film phase became solid-like, while during the phase transition ($9\text{--}17 \text{ \AA}^2$) a conformational change was not observed. For the D/L mixture, a gradual change in the conformational structure was observed during the phase transition, with the change being somewhat accelerated at 9 \AA^2 MMA. These results indicate that there is a correlation between the spectral band shift in crystal-sensitive components and the intermolecular interaction between polymer chains.

Origin of Stereocomplexation of PLA Monolayers at the Air–Water Interface. Time-resolved PA-IRRAS spectra were obtained from the Langmuir films of PLA enantiomers during the compression of the films. It was found that the mixed D/L film exhibited stereocomplexation at the air–water interface due to stereoselective van der Waals interaction, as demonstrated by the band shifts in the $\nu(\text{C=O})$, $\nu_{as}(\text{C-O-C, h})$, $\nu_s(\text{C-O-C})$, and $\nu(\text{C-CH}_3)$ modes. Usually, van der Waals interactions are one of the weakest intermolecular interactions and occur dynamically. However, the interactions in the D/L mixture film occur along the entire chain in a concerted fashion, such that the total energy of interaction is strong enough to lead to considerable band shifts in the IR spectra. Additionally, in order for the polymer chains to have such a strong van der Waals interaction, physical interactions, such as interlocking or interwinding between the D and L types of polymer chains, must be involved so that the altered structure can exhibit strong intermolecular interactions between the polymer chains.¹³

All these observations lead to an obvious question: when does the stereocomplexation between PDLA and PLLA occur? To answer this question, further analysis of both PA-IRRAS spectra and π -A isotherm was carried out. In Figure 5, the $\nu_{as}(\text{C-O-C, h})$ and the $\nu_s(\text{C-O-C})$ modes are shown for the D/L mixed film. The $\nu_{as}(\text{C-O-C, h})$ mode was observed to shift to lower frequency as the phase of the film changed from liquid to solid

due to crystallization. The $\nu_s(\text{C-O-C})$ mode was not affected. This result indicates that there is no crystal transformation from 10_3 - to 3_1 -helix during the film phase transition from liquid- to solid-like film. Therefore, the complexation might occur in the solution state or when the mixed D/L polymer solution forms a thin film on the water surface. However, in the solution state, the D/L mixture IR spectrum was identical to the PLLA spectrum (data not shown). Additionally, the features of the π -A isotherm for the mixed D/L film were significantly different from those of the PLLA film throughout all phases of the films. Therefore, these results suggest that stereocomplexation occurs when the mixed polymer solution forms a thin film on the water subphase. At low compression, this monolayer of stereocomplexed molecules is expanded with a large area per molecule. During compression, the stereocomplexed molecules begin to crystallize resulting in a condensed phase with a reduced area per molecule.

Conclusions

In this study, the origin of the stereocomplexation in PLA enantiomeric monolayers at the air–water interface was investigated. A newly developed PA-IRRAS was employed as a probe to follow the conformational change associated with intermolecular interaction of polymer chains during the compression of the monolayers. Spectroscopic studies revealed that the D/L enantiomeric polymer mixture formed a stereocomplex in the solvent cast film as well as in the 2-D monolayer film at the air–water interface as demonstrated by the distinct difference in the spectra between PLLA and D/L mixed films. Stereocomplexation led to significant band shifts in not only crystal-sensitive components but also amorphous-dependent components in PA-IRRAS spectra. It was also found that the stereocomplex formed when the D/L mixed solution was spread and formed a thin film at the air–water interface before film compression. This means that there is no direct correlation between the stereocomplexation and the compression process for the films. Instead, the compression of the films led to film crystallization. Fourier self-deconvoluted spectra revealed that the film crystallization resulted in a distinct band shift in the crystal-sensitive components only, e.g., the $\nu_{as}(\text{C-O-C, h})$ mode. Moreover, it was found that there is a correlation between the spectral band shift in crystal-sensitive components and the intermolecular interaction between polymer chains. Hence, these results suggest that the newly developed technique of PA-IRRAS is useful for investigating the dynamics of a broad range of monolayer systems at the air–water interface.

Acknowledgment. This work was supported by the National Science Foundation-Nanoscale Interdisciplinary Research Teams (NSF-NIRT), the National Institutes of Health (1R21EB03288-01), and a subcontract from PAIR Technologies LLC (under the NSF STTR program).

LA801747K